ChemComm

Cite this: *Chem. Commun.*, 2012, **48**, 10654–10656

www.rsc.org/chemcomm

COMMUNICATION

Directed patterning of the self-assembled silk-elastin-like nanofibers using a nanomechanical stimulus†

Sara Johnson,[a] Young Koan Ko,[b] Nitinun Varongchayakul,[b] Sunhee Lee,[f] Joseph Cappello,[d] Hamidreza Ghandehari,[de] Sang Bok Lee,[cf] Santiago D. Solares*[g] and Joonil Seog*[b]

Received 25th July 2012, Accepted 11th September 2012
DOI: 10.1039/c2cc35384a

We investigate the effects of the frequency and density of a nanomechanical stimulus on nucleation and growth of silk-elastin-like protein polymer (SELP) nanofibers. Repetitive tappings are crucial to create nucleation areas and a potential molecular level mechanism was proposed. Using this technique mechanically guided nanofiber patterns were successfully created.

Peptide–peptide interactions are essential in the formation of hierarchical biological structures.[1] The major driving forces for self-assembled structures are molecular interactions such as hydrogen bonding, hydrophobic interactions, and electrostatic interactions.[2] Synthetic peptides can be specifically designed to produce well-defined nanostructures by controlling these intermolecular interactions.[3–5] The self-assembly of naturally occurring polypeptides into nanofibrillar structures under certain physiological conditions appears to be a common property of peptides in nature.[6,7] Recently, assembly dynamics of proteins on charged surfaces and mechanical manipulation of individual peptide nanofilaments have been reported.[8,9]

Silk-elastin-like protein polymers (SELPs) are genetically engineered block copolymers made of silk-like blocks (Gly-Ala-Gly-Ala-Gly-Ser) from *Bombyx mori* (silkworm) and elastin-like blocks (Gly-Val-Gly-Val-Pro) from mammalian elastin. At body temperature, the SELP forms a self-assembled hydrogel network which is useful for drug delivery and tissue engineering applications.[5] Recently a two-step self-assembly process of SELPs in aqueous solution and the importance of the ratio of silk-to-elastin blocks in the self-assembly were reported.[10]

[a] *Fischell Department of Bioengineering, University of Maryland, College Park, MD, USA*
[b] *Department of Materials Science and Engineering, University of Maryland, College Park, MD, USA. E-mail: jseog@umd.edu; Fax: +1 301-314-2029; Tel: +1 301-405-1885*
[c] *Department of Chemistry and Biochemistry, University of Maryland, College Park, MD, USA*
[d] *Department of Pharmaceutics and Pharmaceutical Chemistry, University of Utah, UT, USA*
[e] *Department of Bioengineering and Utah Center for Nanomedicine, University of Utah, UT, USA*
[f] *Graduate School of Nanoscience and Technology (WCU), Korea Advanced Institute of Science and Technology, Daejeon, Korea*
[g] *Department of Mechanical Engineering, University of Maryland, College Park, MD, USA*
† Electronic supplementary information (ESI) available. See DOI: 10.1039/c2cc35384a

We discovered that the SELP self-assembles into nanofibrous structures on a hydrophilic negatively charged surface.[11] We also observed that the growth of SELP nanofibers was accelerated and directionally controlled using a nanomechanical stimulus.[12] However, molecular level mechanisms for this mechanically guided self-assembly were not elucidated yet. In this report, we investigate the nucleation area formation by nanomechanical stimulation which can provide fundamental insights on the role of nanomechanical force during transitions from an amorphous state to an ordered state.

The silk-elastin-like protein polymer (SELP-815K) was genetically synthesized using recombinant DNA techniques and characterized as described previously.[13] The frozen 1.2% (wt/wt) solution of SELP-815K in phosphate buffered saline (PBS) was diluted to 5 μg ml^{-1} by mixing with deionized (DI) water. 40 μL of the SELP solution was dispensed on the freshly cleaved mica disk (Ted Pella, Inc., Redding, CA). The samples were incubated for 30 minutes at room temperature. After incubation, the sample was washed with DI water three times (Fig. S1, ESI†) and immediately imaged in DI water using Atomic Force Microscopy (AFM) (MFP-3D, Asylum Research Inc., Santa Barbara, CA). Fig. 1 shows the AFM images of the same area in two consecutive scans. The first scanned image of SELP on mica showed long continuous nanofibers (Fig. S2, ESI†) which were formed during the incubation period (Fig. 1A). In addition, many small heightened areas marked by white arrows were observed throughout the scanned area. We overlaid the first scanned image on the second scanned image of the same area where the heightened area in the first image is shown in grey (Fig. 1B). The comparison of the first and second scanned images clearly showed that new nanofibers grew from the heightened areas in the first scanned image. In the second scanned image (Fig. 1B) newly formed heightened areas indicated with black arrows were observed. They were not present in the first scanned image, indicating that they were formed during the second scan.

Since small heightened areas are strongly correlated with new nanofiber growth, we define those areas as "nucleation areas". The average height of the nucleation areas was 2.2 ± 0.4 nm and the averaged area of individual nucleation area was 868 ± 251 nm^2 (n = 60). The maximum length of the nucleation areas in the horizontal direction (parallel to the scan direction) and vertical direction (perpendicular to the scan direction) was

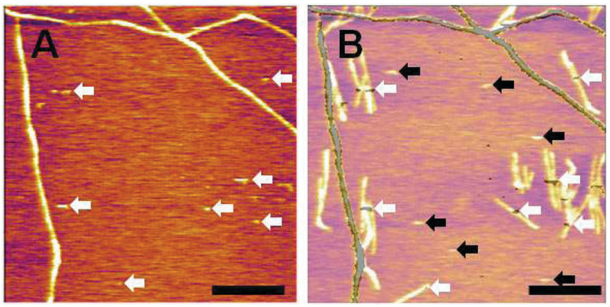

Fig. 1 The identification of SELP-815K nucleation areas during AFM imaging in DI water. (A) The first scanned image with nucleation areas marked with white arrows. (B) The second scanned image of the same area overlaid by the first image to show new nanofiber growth from the nucleation areas identified in the first image. New nucleation areas formed during the second scan are marked with black arrows. The setpoint/free amplitude was 380 mV/400 mV, and tapping force was 2.8 nN. The scan speed and the number of scan lines were 3.34 μm s^{-1} and 256, respectively. The scale bar is 500 nm.

51 ± 11 nm and 28 ± 6 nm, respectively. The aspect ratio (horizontal/vertical length) of the nucleation area was 1.8, indicating that the nucleation area has an elongated shape in the horizontal direction which is the scanning direction.

The effect of tapping frequency on nanofiber self-assembly was investigated at three scan speeds (5, 10 and 15 μm s^{-1}). At one specific scan speed, the same area was repeatedly scanned three times. Fig. 2A shows that the nanofiber coverage increased as the number of scans increased. Interestingly, a significant increase in fiber coverage was noticed between the first and second scans at 5 μm s^{-1}. A comparison of the total nucleation area, the sum of all the nucleation areas, demonstrated that the greatest increase occurred in the first scanned image at 5 μm s^{-1}, consistent with the dramatic increase in nanofiber coverage between the first and the second scanned images (Fig 2B). There was only a marginal increase in the total nucleation area in the second and third scanned images at 5 μm s^{-1}, indicating that the increase in fiber coverage between these scans was mostly due to elongation of existing nanofibers. The total nucleation areas of subsequent scans at 10 and 15 μm s^{-1} also remained low, indicating that lower tapping frequency is less favourable for the formation of nucleation areas, hence nanofiber self-assembly.

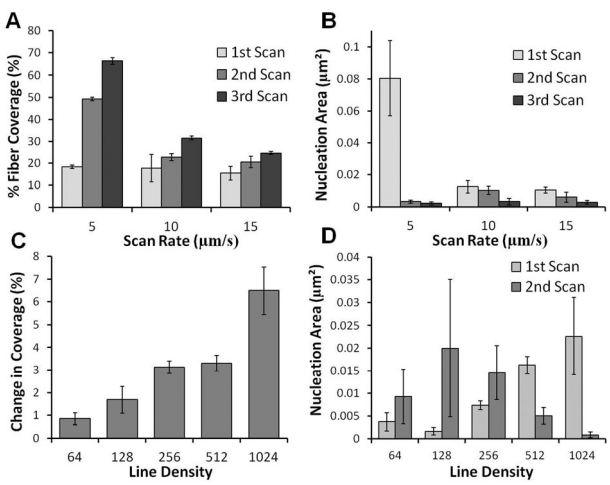

Fig. 2 The effect of the frequency and density of tapping on nucleation and nanofiber coverage. (A) SELP-815K nanofiber coverage (% of surface) in the three consecutively scanned areas at various scan speeds (5, 10, and 15 μm s^{-1}, n = 3). (B) The total nucleation area (μm^2) for the first, second, and third scans at various scan speeds (5, 10, and 15 μm s^{-1}, n = 3). (C) Percent change of SELP-815K nanofiber coverage between the first and second AFM scans at various line densities (64, 128, 256, 512, and 1024 lines per scan, n = 3). (D) The total nucleation area (μm^2) in the first and the second AFM images at various line densities (n = 3).

We also examined the effect of tapping density on nucleation area and nanofiber coverage by changing the number of scan lines. The number of scan lines in the 2 μm × 2 μm area was varied from 64 to 1024. As the number of scan lines increased, the change in nanofiber coverage between the first and second scanned images increased proportionally (Fig. 2C). The total nucleation area formed in the first scan also showed the similar trend, indicating that more nucleation areas were formed as the number of scan lines increased (Fig. 2D) However, the total nucleation area in the second scan did not show any clear dependency on the number of scan lines. Interestingly, the AFM image with 1024 scan lines showed the least total nucleation area in the second scan. This is presumably because SELP-815K is mainly used for nanofiber elongation from nucleation areas created in the first scan, limiting creation of new nucleation areas.

We further studied how consecutive mechanical stimulus affects nucleation area and nanofiber coverage at two different setpoint/free amplitude ratios (Fig. 3). Ratios of 280 mV/400 mV and 320 mV/400 mV were used and the peak forces at each ratio were 6.32 and 5.36 nN respectively.[14] The change in nanofiber coverage at 280 mV/400 mV was greater than that at

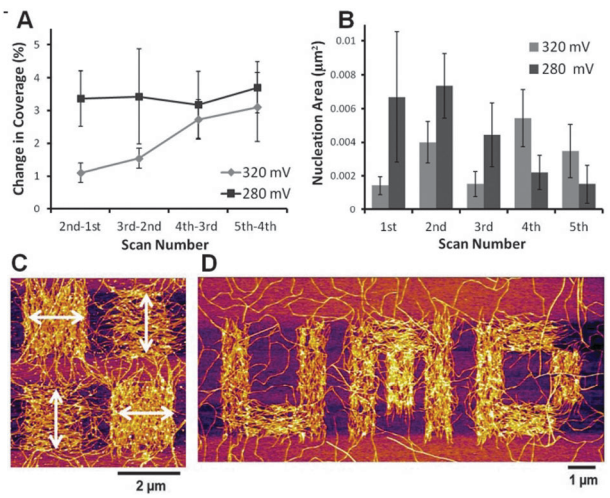

Fig. 3 (A and B) The effect of five consecutive scans on total nucleation area and nanofiber coverage. (A) Percent change of nanofiber coverage between the first and second AFM scans at two setpoint/free amplitude ratios (280/400 mV and 320/400 mV). The x axis label is the difference in nanofiber coverage between the scans (n = 5). (B) The total nucleation area (μm^2) measured at each scan at two setpoint/free amplitude ratios (n = 5). (C and D) Directed patterning of SELP-815K nanofibers using a nanomechanical stimulus. (C) Four 2 μm × 2 μm squares were patterned with the SELP nanofibers by alternating the scanning direction of the tip as indicated by the white arrows. (D) Mechanically guided SELP nanofibers created the "UMD" logo with a 1 μm line width.

320 mV/400 mV during the first few consecutive scans but it became similar after four consecutive scans (Fig. 3A). The total nucleation areas created at 280 mV/400 mV were larger than those at 320 mV/400 mV during the first few scans, consistent with differences in nanofiber coverage (Fig. 3B). The total nucleation area formed at 280 mV/400 mV tended to decrease in the five consecutive scans whereas the total nucleation area formed at 320 mV/400 mV seemed to fluctuate without showing a decreasing tendency. This observation indicates that repeated tapping is one of the key parameters to induce more nucleation area although higher tapping force induced faster and more nanofiber growth in the beginning.

We attempted to create patterns composed of SELP-815K nanofibers using the nanomechanical stimulus. When the 2 μm × 2 μm area was tapped by the AFM tip, a square pattern of nanofibers was generated (Fig. 3C). The white arrows indicate the scanning direction of AFM during stimulation. Newly grown nanofibers were mostly perpendicular to the scanning direction as previously noted. Four square patterns that are composed of SELP nanofibers were successfully created by alternating scan angles by 90°, showing that self-assembly of nanofibers can be locally stimulated with directional control. Mechanically guided nanofiber patterning was further applied to create a more complicated pattern. Fig. 3D shows that the "UMD" logo was successfully patterned on the mica through the nanomechanical stimulus.

In this study, we examined the effects of tapping frequency, density of the mechanical stimulus, and consecutive taps on the nucleation process of SELP-815K nanofibers to obtain fundamental insights on nanomechanically enhanced self-assembly. The fact that most nanofibers grew from the nucleation area shows that the formation of the nucleation area is the rate-limiting step in SELP nanofiber self-assembly. Furthermore, nucleation areas had an elongated shape in the scanning direction, which suggests that shearing force during the scanning has a significant impact on the formation of the nucleation area. We speculate that the scanning directional force caused molecular alignments in the elongated nucleation areas which would direct the SELP nanofiber growth.

The slow scan speed induced more nucleation areas, resulting in more nanofiber growth. At 5 μm s^{-1}, the tapping density in a single line scan is increased three times compared to 15 μm s^{-1}. The significantly increased nucleation area at slower scan speed strongly indicates that a higher tapping frequency is crucial to induce nucleation area formation. The number of scan lines also had a substantial impact on nucleation formation. The nucleation area formed during the first scan was largely proportional to the number of scan lines but this tendency seemed to be reversed in the second scan. The similar trend was also observed in multiple consecutive scans. This implies a few key aspects of the surface facilitated self-assembly process. The quantity of the SELP is limited by the amount of adsorbed SELP during incubation. If more nucleation areas are created during the first scan, there will be less SELP available to create nucleation areas in the next scan. In addition, the formation of the nucleation area in the second scan must compete with nanofiber elongation which is expected to have lower activation energy than nucleation formation. This can further decrease the amount of nucleation area in the second scan. Hence, the self-limiting nature of the material supply and competition between nucleation and elongation are likely to be responsible for the reverse trend in nucleation area formation in the second scan experiment. Furthermore, the increase of total nucleation area in the multiple scanning emphasized the importance of the repetitive tapping in the formation of the nucleation.

When the SELP is adsorbed on mica, it would be expected to be in kinetically trapped states, unable to initiate a nucleation process. The tapping force apparently helps the SELP to overcome the activation energy in a rugged energy landscape so that the SELP can reach a lower energy state.[15] As the AFM tip approaches the SELP adsorbed on mica, the SELP is compressed under the force. At the current tapping force level, it is also possible that the SELP molecule may be picked up by the AFM tip, stretched and collapsed into a new conformational state during the oscillatory motion of the tip (Fig. S3, ESI†).[16] We speculate that this iterative reorganization process may be crucial in nucleation area formation under AFM tapping force. The trial and error model of iterative annealing mechanisms was developed for chaperonin-facilitated protein folding.[17] We show here that arbitrary patterns composed of aligned SELP nanofibers can be created using a nanomechanical stimulus. Improved control over nuclei location and nanofiber orientation would make this approach very unique and powerful to prepare nanofiber patterned functional devices.

Notes and references

1 S. Zhang, *Nat. Biotechnol.*, 2003, **21**, 1171–1178.
2 T. P. Knowles, A. W. Fitzpatrick, S. Meehan, H. R. Mott, M. Vendruscolo, C. M. Dobson and M. E. Welland, *Science*, 2007, **318**, 1900–1903.
3 S. Ramachandran, Y. Tseng and Y. B. Yu, *Biomacromolecules*, 2005, **6**, 1316–1321.
4 J. D. Hartgerink, E. Beniash and S. I. Stupp, *Science*, 2001, **294**, 1684–1688.
5 M. Haider, J. Cappello, H. Ghandehari and K. W. Leong, *Pharm. Res.*, 2008, **25**, 692–699.
6 C. M. Dobson, *Nature*, 2003, **426**, 884–890.
7 W. Hwang, S. Zhang, R. D. Kamm and M. Karplus, *Proc. Natl. Acad. Sci. U. S. A.*, 2004, **101**, 12916–12921.
8 C. L. Chen, K. M. Bromley, J. Moradian-Oldak and J. J. DeYoreo, *J. Am. Chem. Soc.*, 2011, **133**, 17406–17413.
9 F. C. Zhang, F. Zhang, H. N. Su, H. Li, Y. Zhang and J. Hu, *ACS Nano*, 2010, **4**, 5791–5796.
10 X. X. Xia, Q. B. Xu, X. Hu, G. K. Qin and D. L. Kaplan, *Biomacromolecules*, 2011, **12**, 3844–3850.
11 W. Hwang, B. H. Kim, R. Dandu, J. Cappello, H. Ghandehari and J. Seog, *Langmuir*, 2009, **25**, 12682–12686.
12 J. Chang, X. F. Peng, K. Hijji, J. Cappello, H. Ghandehari, S. D. Solares and J. Seog, *J. Am. Chem. Soc.*, 2011, **133**, 1745–1747.
13 R. Dandu, A. Von Cresce, R. Briber, P. Dowell, J. Cappello and H. Ghandehari, *Polymer*, 2009, **50**, 366–374.
14 S. D. Solares, J. Chang, J. Seog and A. U. Kareem, *J. Appl. Phys.*, 2011, **110**, 094904.
15 D. Thirumalai and D. K. Klimov, *Methods Mol. Biol.*, 2007, **350**, 277–303.
16 P. E. Marszalek, H. Lu, H. Li, M. Carrion-Vazquez, A. F. Oberhauser, K. Schulten and J. M. Fernandez, *Nature*, 1999, **402**, 100–103.
17 M. J. Todd, G. H. Lorimer and D. Thirumalai, *Proc. Natl. Acad. Sci. U. S. A.*, 1996, **93**, 4030–4035.

